Band structure and Fermi surface of hcp ferromagnetic cobalt

Francisco Batallan and Izio Rosenman
Groupe de Physique des Solides de l'Ecole Normale Supérieure, Paris VII, Tour 23, 2 place Jussieu, 75221 Paris Cedex 05, France*

C. B. Sommers
Centre Européen de Calcul Atomique et Moléculaire,† Bât. 506, Campus d'Orsay-91401 Orsay, France
(Received 3 June 1974)

A Korringa-Kohn-Rostoker first-principles computation of the band structure of ferromagnetic hcp cobalt is reported. A muffin-tin potential and a Kohn-Sham exhange-correlation potential were used in conjunction with a rigid exchange splitting. Twelve energy bands in 1/24th of the hcp Brillouin zone were calculated as well as the density of states and the Fermi surface. The exchange splitting was found to be 1.39 eV and a total density of states at the Fermi level of 15.61 electrons/(atom Ry). The spin-orbit coupling constant ξ_{3d} has been computed and is equal to 6×10^{-3} Ry. The essential features of the band structure agreed with the requirements of the itinerant-electron model of ferromagnetism of the Stoner-Wohlfarth theory. Our resulting density of states was able to explain the available photoemission data. The calculated Fermi surface is in good agreement with the de Haas–van Alphen experiments, particulary for the neck of the point Γ in the spin-up Fermi surface. The spin-orbit interaction has been taken into account in a qualitative way in order to explain the orbits around L in the spin-down Fermi surface. A comparison with the existing experimental data has permitted us to estimate the mass enhancement due to many-body effects at the Γ neck as 1.04, resulting in a value of 0.81 for the electron-magnon contribution.

I. INTRODUCTION

Among the $3d$ ferromagnetic transition metals, iron, nickel, and cobalt, the first two have been extensively studied with regard to experiment and theory in order to understand the origin of their ferromagnetism as well as the validity of the itinerant-electrons model.[1] The experimental Fermi surface (FS) data were thus very relevant. These experiments, which included the study of the de Haas–van Alphen (dHvA) effect and that of the magnetoresistance and the cyclotron resonance, have shown the presence of some particular phenomena related to ferromagnetism; i.e., spin-dependent magnetic breakdown, spin-mixed FS portions, and effects related to the combined action of the exchange and the spin-orbit coupling. A general and up-to-date review of the problems and data related to the FS of the ferromagnetic transition metals has been recently published by Gold.[2]

Unlike iron and nickel, cobalt has received little attention until very recent years. The lack of experimental work, mainly due to the difficulty of obtaining good single crystals, has been fulfilled in the last few years by FS studies.[3-7]

Our interest in the band structure of hcp cobalt stemmed from the fact that we have ourselves, over the past few years, performed a detailed set of dHvA and magnetoresistance experiments,[3-6] and thus had need of a detailed band structure in order to understand our results.

The first[8-11] band-structure computations on cobalt were mainly limited to the determination of the density of states in order to interpret the then existing photoemission data.[12,13] Wohlfarth[14] in particular was interested in the band magnetism and has reviewed the properties of cobalt in the light of itinerant-electrons ferromagnetism. Connolly[15] was the first to publish some results on the FS. Using an augmented-plane-wave (APW) method and an optimized spin-dependent potential, he was able to calculate a band structure which, however, was limited to the determination of only the majority-electrons FS (FS ↑). Later, Wakoh and Yamashita[16] made a complete computation of the energy bands and FS. They used the Korringa-Kohn-Rostoker (KKR) method with a rigid exchange. Recently, Ishida[17] has extended Mueller's interpolation scheme to the hcp structure and has applied it in order to obtain the FS of cobalt.

As will be seen later, none of the published band structures and FS models were capable of explaining the experimental results, particularly those of the dHvA effect, so that we were forced to make a new computation, which is presented in this paper. This was an *ab initio* KKR computation of the band structure of hcp ferromagnetic cobalt with a rigid exchange.

In Sec. II we explain the theoretical assumptions and the principles of our computation. Section III is devoted to the presentation of our results for the band structure, the density of states, and the FS.

On the basis of these results, we present in Sec. IV some conclusions concerning the band magnetism in cobalt. Section V is concerned with the comparison of the experimental results, both those related to the density of states and those related to the detailed structure and shape of the FS. In Sec. VI, we evaluate the many-body mass enhancement in cobalt, including the electron-magnon interaction. And finally, before concluding, we discuss the basic hypotheses and validity of this band structure computation.

II. THEORY

We have calculated the band structure and several associated electronic properties of hcp ferromagnetic cobalt, using a formalism and a KKR computer program developed by one of the authors.[18] The program was capable of calculating the energy bands both relativistically as well as nonrelativistically at arbitrary points in the hcp Brillouin zone (BZ) (see Fig. 1). At points or in directions of high symmetry we used the irreducible representations of the appropriate point groups[19] which enabled us to connect all the bands without ambiguity. The approximations made were as follows.

(a) Muffin-tin potential. A spherically symmetric potential centered about each atomic site and a constant potential V_0, resulting from an averaged $V(r)$ in the interstitial region was used. This choice of potential is especially appropriate for the close-packed metals where the interstitial volume is small and the nonspherical contribution from $V(r)$ can be neglected.

(b) Kohn-Sham exchange-correlation potential. The local density exchange-correlation potential due to Kohn and Sham[20] was used as we did not wish to introduce any *ad hoc* parameter.

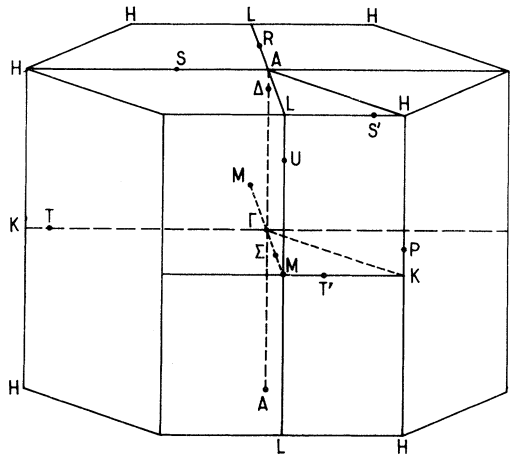

FIG. 1. hcp Brillouin zone.

(c) Rigid-exchange-band approximation. We have used the hypothesis of a rigid exchange between electrons of opposite spin in the Hamiltonian for the determination of the spin-up (majority electrons) and spin-down (minority electrons) energy bands. Thus we have two systems of identical bands separated in energy by the exchange splitting. This can be represented as one set of energy bands with two Fermi levels which were determined by rigidly shifting the bands in energy in accordance with the number of occupied electron states $n\uparrow$ or $n\downarrow$ as obtained by the experimentally measured Bohr magneton number.

Starting from an atomic charge density $\rho_a(r)$ generated from a Hartree-Fock-Slater program of Desclaux,[21] with an atomic configuration $3d^7 4s^2$, we were able to create a crystal potential $V_X(r)$ according to approximations (a) and (b). The $E(k)$ were then determined in 196 nonequivalent points of the $\frac{1}{24}$ irreducible part of the BZ. This enabled us to calculate a density of states and a FS for both spins. The numerical values of the different parameters of cobalt used in this calculation are listed in Table I.

III. RESULTS OF CALCULATION

A. Energy bands

As we have said before, the two identical systems of bands resulting from the rigid exchange hypothesis (split band model) can be represented by only one system of bands with two Fermi levels separated by the exchange splitting. In Fig. 2 we represent this system of energy bands for the di-

TABLE I. Atomic and crystallographic parameters used in the present work.

Atomic parameters Configuration $3d^7 4s^2$	
Orbital	Energy (Ry)
$1s_{1/2}$	$-2.783\,492\,2\times10^2$
$2s_{1/2}$	$-3.295\,451\,2\times10$
$2p_{1/2}$	$-2.862\,669\,4\times10$
$2p_{3/2}$	$-2.808\,351\,5\times10$
$3s_{1/2}$	$-3.748\,986\,4$
$3p_{1/2}$	$-2.459\,271\,5$
$3p_{3/2}$	$-2.390\,714\,5$
$3d_{3/2}$	$-3.223\,081\,3\times0.1$
$3d_{5/2}$	$-3.152\,420\,5\times0.1$
$4s_{1/2}$	$-2.437\,642\,0\times0.1$
Crystal parameters	
$a=7.446\,078$ a.u.	
$c=4.743\,268$ a.u.	
$a/c=1.633\,067$	

rections of high symmetry in the irreducible part of the BZ. The energy values are given in Rydbergs. The labeling of the single group representations is that of Herring.[19] For sake of clarity, we have suppressed the letters in his notation and exhibit only the numerical subscripts on each band.

There are nine electrons per atom and two atoms per BZ, giving a total of 18 bands, of which ten are d like. The d bands extend over a range of energies from −1.22 to −0.85 Ry.

We did not explicitly calculate the wave-function coefficients, however, the atomic like nature of some of the bands can be deduced from symmetry considerations. At Γ, the lowest level Γ_{1+} is s like. The Γ_{4-} state just above is a mixture of s and d functions while the remaining states are all rather purely d like, except for Γ_{3+} which is made up of p functions.

The Fermi levels for both spins, $E_F\uparrow$ and $E_F\downarrow$, are also shown in Fig. 2, while the numerical values of $E(k)$ for the points of high symmetry are listed in Table II.

B. Density of states and Fermi levels

The density of states $N(E)$ is shown in Fig. 3. The three large peaks centered about energies of −1.08, −0.98, and −0.85 Ry are those corresponding to the d bands. The Fermi level for paramagnetic cobalt, E_F, was obtained by filling the bands (starting from the lowest energy) until nine electrons/atom were accounted for. This gave

$$E_F = -0.8766 \text{ Ry}.$$

The corresponding Fermi levels for the spin-up and spin-down states were determined from the Bohr-magneton number (1.56) found experimentally, i.e.,

$$n\uparrow + n\downarrow = 9\,, \quad n\uparrow - n\downarrow = 1.56\,,$$

giving

$$n\uparrow = 5.28\,, \quad n\downarrow = 3.72\,,$$

where $n\uparrow$ and $n\downarrow$ are the numbers of majority and minority electrons/atom. The resulting Fermi energies were found to be

$$E_F\uparrow = -0.8295 \text{ Ry}\,, \quad E_F\downarrow = -0.9318 \text{ Ry}\,,$$

giving an exchange splitting

$$\Delta E = E_F\uparrow - E_F\downarrow = 0.1023 \text{ Ry} = 1.39 \text{ eV}.$$

The Fermi levels have been superimposed on the density of states (DOS) curve.

The fact that $E_F\uparrow$ falls in a region where the DOS is small and due to s- and p-type bands, implies that cobalt is a strong ferromagnet. The $E_F\downarrow$, on the other hand, falls in the region where the DOS is relatively large due to the presence of d-like bands. In Fig. 4 we represent the total DOS of the ferromagnetic state. This is obtained by superimposing the DOS for each spin orientation, relative to the Fermi level.

The numerical values of the Fermi levels and density of states are given in Table III as well as other parameters related to the band structure.

C. Fermi surfaces

Once having calculated the Fermi levels for both spins, we were able to determine the corresponding Fermi surfaces.

Figure 5 shows the principal cross sections of the spin-up Fermi surface (FS↑) (dashed lines). In the simple zone scheme (see Sec. III D) the FS↑ consists of two parts: (a) a quasihyperboloid, e_{12},[22] centered about the ΓA axis and giving rise to a neck; and (b) an anisotropic ball, e_{11}, elongated along ΓA with protuberances of hexagonal symmetry in the ⟨1010⟩ directions.

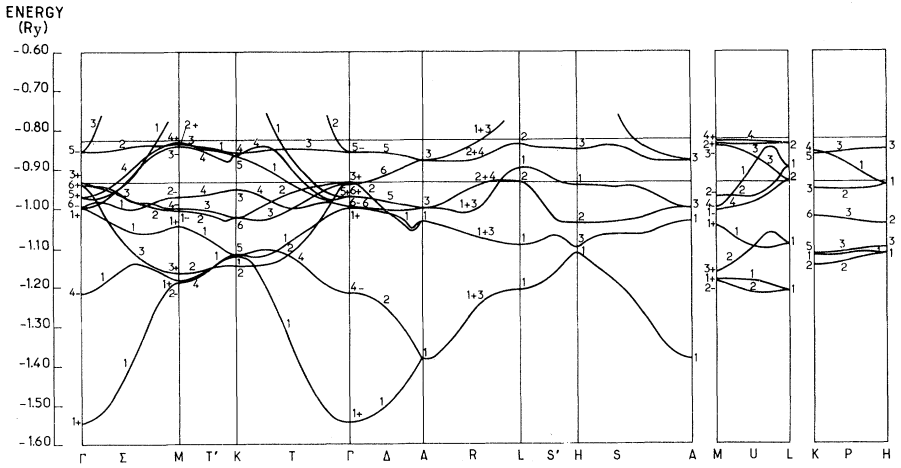

FIG. 2. Energy bands of hcp cobalt in the high-symmetry directions in the split-band model. The two Fermi levels of majority ($E_F\uparrow$) and minority ($E_F\downarrow$) electrons are also shown.

The principal cross sections of the spin-down Fermi surface (FS↓) are also shown in Fig. 5 (solid lines). This surface consists of: (a) three pockets centered around Γ; the smallest, h_{10}, has a hole character, while the other two e_9 and e_{10} have an electron character; (b) a multiconnected monster h_9; (c) a hole surface, centered around L and composed of intersecting pockets (h_5, h_6, and h_7) due to accidental degeneracies.

Fig. 6 represents a schematic drawing of the different portions of the cobalt FS.

TABLE II. Representations and energy values (in Ry) for the high-symmetry points in the Brillouin zone.

Reps	Energy (Ry)
Γ_{1+}	−1.545 921
Γ_{4-}	−1.215 111
Γ_{1+}	−0.998 179
Γ_{6-}	−0.994 449
Γ_{5+}	−0.968 452
Γ_{6+}	−0.937 191
Γ_{3+}	−0.929 153
Γ_{5-}	−0.854 398
K_2	−1.144 663
K_1	−1.119 883
K_5	−1.115 618
K_6	−1.022 225
K_3	−0.950 346
K_5	−0.862 001
K_4	−0.856 363
H_1	−1.114 853
H_3	−1.100 234
H_2	−1.037 217
H_1	−0.940 070
H_3	−0.848 826
A_1	−1.382 834
A_1	−1.032 904
A_3	−0.998 528
A_3	−0.877 927
M_{2-}	−1.187 126
M_{1+}	−1.181 794
M_{3+}	−1.163 300
M_{1+}	−1.045 278
M_{1-}	−1.005 339
M_{4-}	−0.999 241
M_{2-}	−0.970 365
M_{3-}	−0.841 485
M_{2+}	−0.837 541
M_{4+}	−0.830 471
L_1	−1.209 683
L_1	−1.092 094
L_2	−0.930 173
L_1	−0.896 495
L_2	−0.834 983

D. Spin-orbit coupling and relativistic effects

If we wish to include relativistic effects in our ferromagnetic band calculation, we are faced with a more difficult problem than is usually the case in that the exchange Hamiltonian does not commute with that of the spin-orbit interaction. This arises because the spin-orbit coupling ignores the well-defined spin orientation character imposed on the bands by the exchange operator, and produces bands of mixed spin.

As a result of this situation, we could not directly perform a relativistic ferromagnetic computation. However, our formalism[18] permitted us to calculate relativistic paramagnetic energies.

In order to estimate the effects of spin-orbit coupling, we have computed, at the Γ point the relativistic paramagnetic energies, with their corresponding symmetries. This made it possible to get both the shift and the splitting of the bands in the relativistic case with reference to the nonrelativistic case (Fig. 7). The shift is not rigid, depending mostly on the s- or d-like character of the wave functions. Its effect is to enlarge the energy difference between the s and d bands. The splitting of the bands is exclusively due to the spin-orbit interaction term in the Hamiltonian.[23]

At the Γ point, the splitting concerns almost pure d states. If we assume that this is the exclusive character of the wave functions it is then possible to compute the spin-orbit coupling by perturbation theory with the following Hamiltonian:

$$H_{s-o} = \tfrac{1}{2}\xi_{3d}\vec{l}\cdot\vec{\sigma},$$

where ξ_{3d} is a constant.

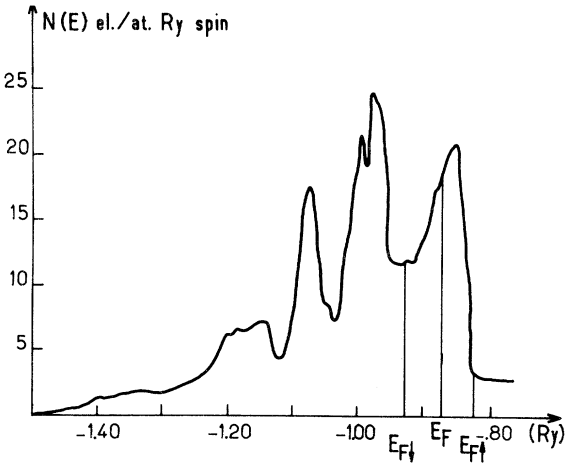

FIG. 3. Density of states in the split-band model with the two Fermi levels $E_F\uparrow$ and $E_F\downarrow$. E_F represents the paramagnetic Fermi level.

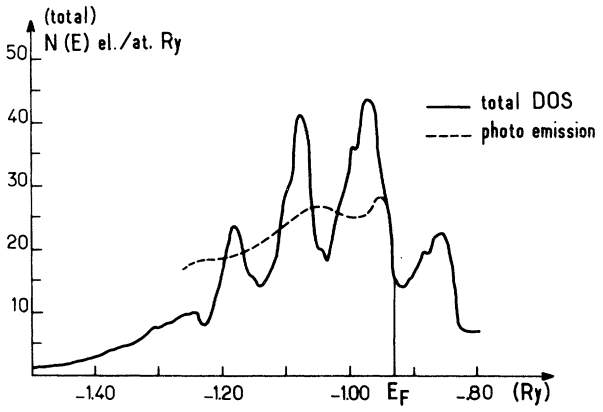

FIG. 4. Total density of states. The ferromagnetic Fermi level is represented by E_F. The dashed line is the energy distribution of photoemitted electrons after Eastman.

The identification of the splitting obtained in the relativistic computation with that obtained from perturbation theory, results in a value of

$$\xi_{3d} = 6\times10^{-3}\ \text{Ry}\,.$$

Values of 6×10^{-3} Ry and 5×10^{-3} Ry have been found, respectively, for nickel[24] and iron.[25]

A problem related to the relativistic computation deserves attention at this time. It concerns the type of BZ in which the results must be represented.

Indeed, in a nonrelativistic computation the ALH plane of the BZ is degenerate. It is not a Bragg reflection plane, and the results must be represented in the double BZ. However, in the presence of spin-orbit coupling the degeneracies on the ALH planes are suppressed,[26] except on the AL line, so that we must use the simple BZ scheme. Falicov and Ruvalds[27] have studied this problem in detail by considering the spin-orbit coupling and the exchange in the presence of an external magnetic induction $\vec{B}$. They found that the only degeneracies due to symmetry are at the points A and L. Accidental degeneracies are possible, only when $\vec{B}$ is parallel to a symmetry direction. In this case, they occur in a plane perpendicular to $\vec{B}$ or on a line parallel to $\vec{B}$.

As our computation was nonrelativistic, the appropriate representation would have been the double BZ. Nevertheless, we have used the simple BZ as it is needed for the comparison of our FS with the experimental results.

IV. BAND MAGNETISM

As has been mentioned above, we have computed the ferromagnetic band structure of cobalt by introducing a rigid exchange obtained from the value of the experimental Bohr magneton number. It is clear that from this type of computation no conclusion can be drawn about the origin of ferromagnetism in cobalt. It is therefore important, in order to test the internal consistency of our band model, to analyze how the ferromagnetic nature of cobalt is reflected in the results of our computation. As far as ferromagnetism is concerned, we can define three energy parameters which characterize the band structure taken as a whole.

(a) The width of the d bands, W, is the energy difference between the top and the bottom of the d bands:

$$W = E_{M_{4+}} - E_{\Gamma_{4-}}\,;$$

(b) the exchange splitting (cf. Sec. III B)

$$\Delta E = E_F\uparrow - E_F\downarrow\,;$$

(c) the parameter Δ defined as the energy difference between the spin-up Fermi level $E_F\uparrow$ and the top of the d bands:

$$\Delta = E_F\uparrow - E_{M_{4+}}\,.$$

The numerical values of these parameters are given in Table III.

TABLE III. Band-structure parameters obtained from this calculation.

Name	Symbol	Units	Value
Paramagnetic Fermi level	E_F	Ry	−0.8766
Majority Fermi level	$E_F\uparrow$	Ry	−0.8295
Minority Fermi level	$E_F\downarrow$	Ry	−0.9313
Density of states at E_F	$N(E_F)$	electrons/(atom Ry spin)	17.26
Density of states at $E_F\uparrow$	$N(E_F\uparrow)$	electrons/(atom Ry spin)	4.29
Density of states at $E_F\downarrow$	$N(E_F\downarrow)$	electrons/(atom Ry spin)	11.32
Width of the d bands	W	Ry	0.3846
Ferromagnetic exchange	ΔE	Ry	0.1023
Δ parameter	Δ	Ry	0.0010
Effective interaction energy	I	Ry	0.0656

A positive Δ, means that $E_F\uparrow$ intersects only the s-p bands, and that the metal is a strong ferromagnet. On the other hand, if Δ is negative, $E_F\uparrow$ also intersects the d bands. Since these bands will not be completely filled, the metal will be a weak ferromagnet.

In our case, Δ is positive, which implies that cobalt is a strong ferromagnet; however, the value of Δ is very small, of the same order of magnitude as the computational error, so that cobalt is at the limit of strong and weak ferromagnetism.

In the Stoner-Wohlfarth theory of magnetism,[1,28] an effective interaction energy between itinerant electrons I, is defined by the relation

$$I = \Delta E/(n\uparrow - n\downarrow),$$

while Kanamori[29] has introduced an effective polarization energy U_{eff}. The above defined I is something like U_{eff} divided by the effective number of d bands. Two inequalities based on these definitions can be established in relation to the existence of ferromagnetism:

(a) $I \times N(E_F) > 1$,

where $N(E_F)$ is the density of states per spin at the paramagnetic Fermi level E_F. This is the Stoner criterion for ferromagnetism.[1]

(b) $U_{\text{eff}} < W$;

this relation fixes the upper limit of the polarization energy, which is given by the width of the d bands. When this relation is expressed in terms of I, we find, taking into account the $5d$ bands:

$$I/W < 0.2.$$

In Table IV we have represented the values of I, W, $IN(E_F)$ and I/W found by the present calculation, as well as the corresponding values for iron and nickel. $IN(E_F)$ and I/W express the existence of ferromagnetism and are more or less independent of the band structure. From Table IV it can be seen that our band model is in agreement with the two inequalities. This shows that by imposing a rigid exchange, as we have done, we find a stable ferromagnetic state. Moreover, the value of $IN(E_F)$ is in excellent agreement with that of nickel and iron, also showing the internal coherence of our model.[14]

The fact that I/W is approximately constant for the three metals suggests a possible common origin for ferromagnetism in the three cases.

V. COMPARISON WITH EXPERIMENT

We will first analyze the results related to the density of states and then proceed to a discussion of the properties depending on the FS topology.

A. Photoemission

Eastman[13] has been able to analyze his photoemission data of cobalt on the basis of the so-called nondirect transition model. He concludes that the optical density of states in the conduction bands is practically constant for energies greater than 5 eV above the Fermi level, so that the energy distribution of the photoemitted electrons observed $N(E, \omega)$ is proportional to the DOS of the valence bands. Figure 4 shows the superposition

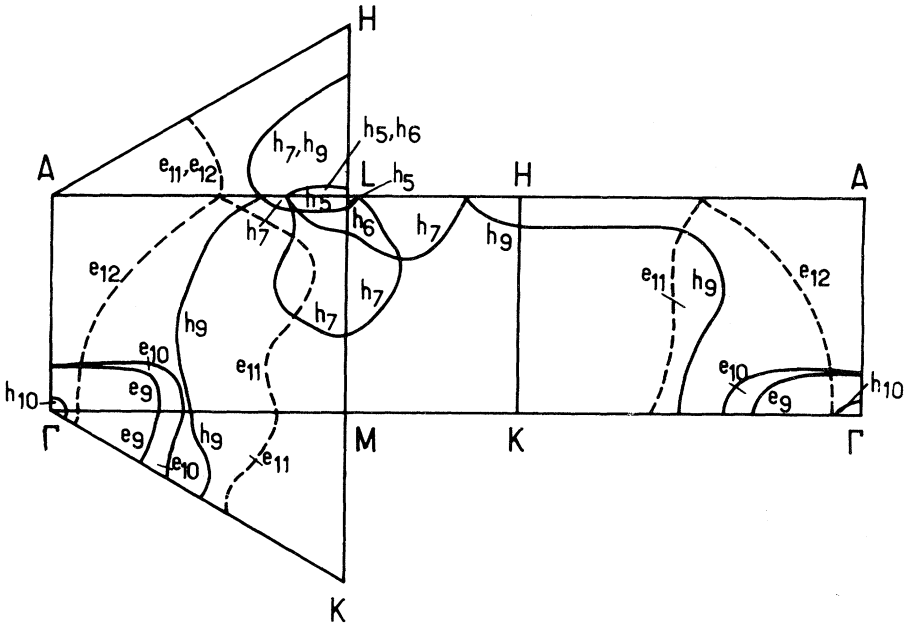

FIG. 5. Cross sections of the majority (dashed lines) and minority (full lines) Fermi surfaces in the principal symmetry planes.

of $N(E, \omega)$ of Eastman (dashed line) with our total DOS. The overall structure of the two curves is approximately the same. The difference in energy between the two large peaks is found by Eastman to be 0.095 Ry, whereas we find 0.100 Ry. However, our curve is shifted rigidly by 0.02 Ry away from the Fermi level with respect to the experimental results. This slight difference can possibly be attributed to the rather crude way in which we have just compared the DOS to the data. However, no detailed computation has as yet been made.

B. Specific heat

The electronic specific heat coefficient γ_{th} calculated in the one-electron model is

$$\gamma_{\text{th}} = \tfrac{1}{3}\pi^2 k_B^2 [N(E_F\uparrow) + N(E_F\downarrow)] .$$

This gives

$$\gamma_{\text{th}} = 6.48 \times 10^{-4} \text{ cal/mole } ^\circ\text{K}^2 .$$

The value γ_{expt} found from specific-heat measurements is[30]:

$$\gamma_{\text{expt}} = 11.3 \times 10^{-4} \text{ cal/mole } ^\circ\text{K}^2 .$$

As it is well known, γ_{expt} includes many-body interactions.[31] Conversely, from γ_{expt} and γ_{th} we can evaluate these effects. In order to facilitate this, we introduce the parameter λ given by

$$\gamma_{\text{expt}}/\gamma_{\text{th}} = 1 + \lambda .$$

We then find

$$\lambda = 0.74 .$$

The many-body interactions will be discussed in detail in Sec. VI.

C. Spin-up Fermi surface (FS↑)

The FS↑ is composed of two large portions (cf. Sec. III C), one of which has a neck centered about the Γ point. The cross-sectional area of this neck is very sensitive to the position of $E_F\uparrow$. We have therefore studied in detail the variation of the area $\mathcal{A}$ as a function of energy near $E_F\uparrow$.

A by-product of this calculation is the band mass, given by

$$\frac{m_b}{m_0} = \frac{h^2}{2\pi} \frac{\partial \mathcal{A}}{\partial E}\bigg|_{E=E_F\uparrow} .$$

For an $E_F\uparrow = -0.8295$ Ry (see Sec. III B) we have

$$\mathcal{A}\langle 0001\rangle = 1.36 \times 10^{-2} \text{ a.u.}$$

and

$$(m_b/m_0)\langle 0001\rangle = 0.107 .$$

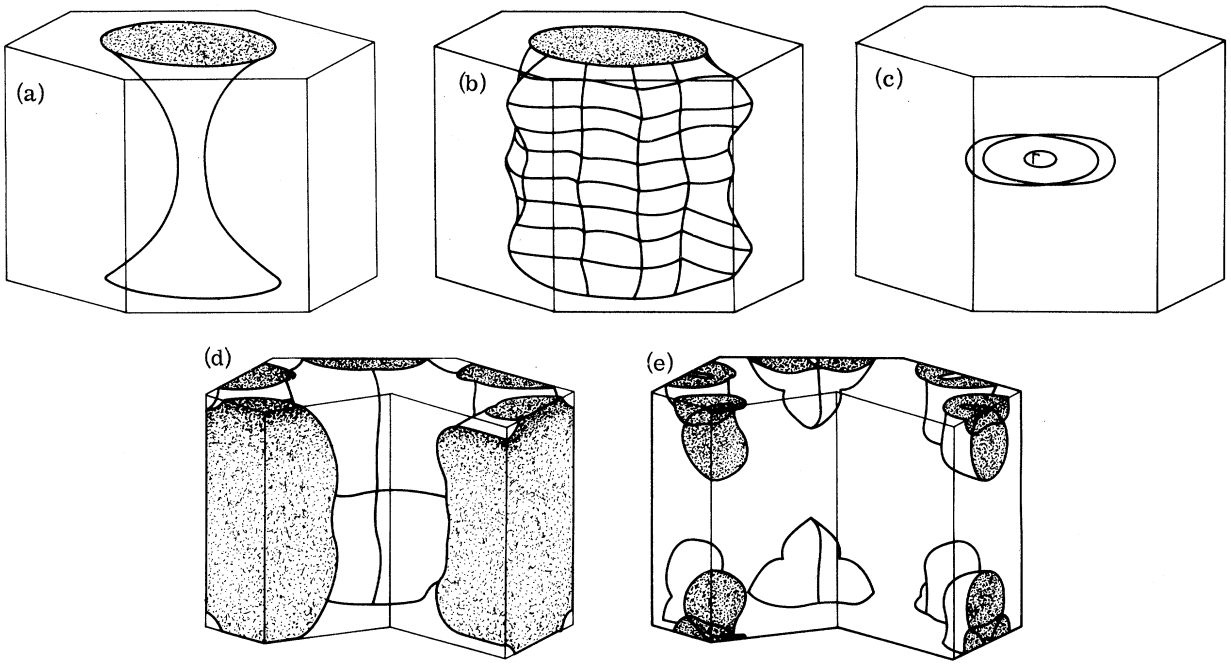

FIG. 6. (a) Majority-electron Fermi surface: the e_{12} hyperboloid with the neck at Γ. (b) Majority-electron Fermi surface: the e_{11} ball. (c) Minority-electron Fermi surface: the three pockets centered around $\Gamma(h_{10}, e_9$, and $e_{10})$. (d) Minority-electron Fermi surface: the h_9 monster. (e) Minority-electron Fermi surface: the interlaced hole surface around L (h_5, h_6, and h_7).

The experimental value as found by the dHvA effect[3] is

$$\mathcal{A}_{\text{expt}}\langle 0001\rangle = 0.989 \times 10^{-2} \text{ a.u.}.$$

If we use the value of $\mathcal{A}_{\text{expt}}$ as a parameter in order to find the Fermi level, we get

$$E_F\uparrow = 0.8346 \text{ Ry}$$

and

$$(m_b/m_0)\langle 0001\rangle = 0.098 .$$

Thus a shift of 0.005 Ry in $E_F\uparrow$ results in a 30% variation in $\mathcal{A}$ but only a 5% variation in m_b/m_0. The reason for this large relative change in area but not a corresponding change in mass is due to the fact that the neck is formed from the bottom of the s-p bands.

This neck at Γ connects two large portions of the FS and makes possible the existence of open orbits in the $\langle 0001\rangle$ direction. These orbits have been observed by magnetoresistance[6] within a 5° angular spread about $\langle 0001\rangle$ which is in very good agreement with our theoretical prediction.

We have also predicted in our hcp cobalt FS other open orbits about $\langle 0001\rangle$ but with a much larger angular spread than those arising from the Γ neck. These orbits have not as yet been observed.

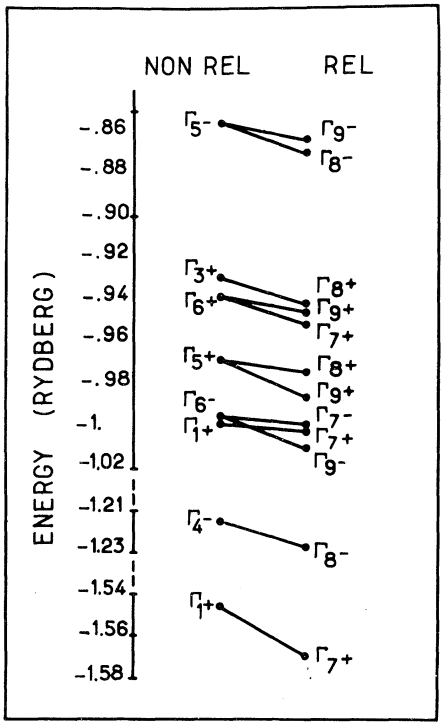

FIG. 7. Comparison between the relativistic and nonrelativistic paramagnetic energy levels at the Γ point.

In Fig. 8 we compare our FS results (1) in the ΓALM plane with those of several others, namely, Wakoh and Yamashita (2) and Connolly (3).

Wakoh and Yamashita, as well as Ishida do not find the neck at Γ. Connolly, on the other hand, finds this neck but with a cross-sectional area four times larger than ours, and centered about Γ_{3+} instead of Γ_{5-}. He also finds another neck in the U direction which we do not find.

Connolly also pointed out that the FS↑ of fcc cobalt (which is identical to that of the noble metals and to the FS↑ of nickel) resembled the FS↑ of hcp cobalt in that it has a neck at the L point. This is topologically equivalent to the Γ neck of the hcp phase.

D. Spin-down Fermi surface (FS↓)

As we have seen in Sec. III C the FS↓ is composed of three pockets h_{10}, e_9, e_{10} centered around Γ, a multiconnected monster h_9, and three intersecting pockets h_5, h_6, and h_7 centered around L.

The contact points between the three pockets around L are the result of accidental degeneracies at the Fermi level between states of even and odd symmetry.

In the presence of the spin-orbit (s-o) interaction, these degeneracies are suppressed everywhere but on the AL line and the connectivity of the FS changes. Hence we see that it is necessary to take into account the s-o interaction in order to get a realistic image of the FS. However, since a relativistic ferromagnetic band computation is not feasible (cf. Sec. III D), we will consider only the accidental degeneracies around L with the aid of simple symmetry arguments by remarking that the s-o interaction implies the replacement of the simple crystallographic group with that of the double group. The R and U lines, around L, have only one extra representation, so that in presence of s-o interaction, there are no band crossings in these directions.

TABLE IV. Parameters related to band magnetism in cobalt, iron, and nickel.

	I (eV)	W (eV)	IN (E_F)	I/W
Co	0.89	5.2	1.13	0.17
Fe[a]	0.97	6.8	1.1	0.14
Ni[b]	0.62	4.0	1.2	0.16

[a] J. F. Cornwell, D. H. Hum, and K. C. Wong, Phys. Lett. A 26, 365 (1968).

[b] E. P. Wohlfarth, *Proceedings of the Nottingham Conference on Magnetism* (Institute of Physics and the Physical Society, London, 1964), p. 51.

The s-o interaction also has the effect of changing the shape of the bands, but this effect is important only for small FS portions, namely, around L.

From these considerations we conclude that the resulting FS↓ is topologically equivalent to that given in Fig. 9. Around L, the FS↓ will be composed of three hole pockets: h_5 which is ellipsoidal; h_6 which is dumbbell shaped, and h_7 which is a large oval-shaped surface.

This FS↓ portion around L resembles that of hcp rhenium as computed by Mattheiss.[32] This is not surprising since cobalt has 7.44 spin-down electrons and rhenium has 7 conduction electrons.

The preceding remarks make it possible to identify the dHvA frequencies. The α and ϵ frequencies[3-5] can be attributed to the h_5 and h_6 pockets around L in the FS↓. The symmetry of these dHvA frequencies is compatible with the pockets centered about the point L. The cross sections corresponding to these frequencies are of the same order of magnitude as those found by our model. A quantitative analysis is impossible because there is still another effect, not yet considered, which comes in addition to the mentioned s-o interaction: this is the combined action of the s-o interaction and the exchange in the presence of a magnetic induction $\vec{B}$, which suppresses degeneracies. This combined interaction has the effect of modulating the bands as a function of the magnetic induction orientation, and changes the apparent shape of the pockets near the degeneracy points. Hodges, Stone, and Gold,[33] using these arguments, have been able to explain the anomalous angular variation of the dHvA frequency corresponding to the d-band pocket near the X point in the FS↓ of nickel. This phenomenon is a consequence of the symmetry breaking of the double group for a ferromagnet in the presence of a magnetic induction $\vec{B}$.

We have seen that in the FS↓ there is also a multiconnected monster h_8 which permits the existence of open orbits along the $\langle 10\bar{1}0\rangle$ direction. These orbits have been observed by Coleman *et al.*[7] in magnetoresistance experiments. The monster also permits the existence of open orbits in the $\langle 0001\rangle$ direction, but no such orbits have as yet been reported.

The FS↓ has been previously calculated by Wakoh and Yamashita[16] and by Ishida.[17] Both groups find the same type of FS↓, which differs from our model around L. Indeed, in their computations the lowest L_2 symmetry band is below E_F↓, (whereas in ours it is just above), such that their computations give rise to a FS↓ around L composed of two interlaced pockets. In the presence of the s-o interaction this results in two pockets, one centered around U and the other around L, a situation quite different from ours.

E. Spin hybridization and observed Fermi surface

We have up to this point represented our ferromagnetic band structure by one set of bands with two Fermi levels. We now wish, however, to consider a representation where we have one Fermi level with two shifted sets of energy bands, resulting in numerous crossings between bands of opposite spin.

In the presence of the s-o interaction spin is no longer a good quantum number (cf. Sec. III D). The s-o interaction mixes bands of opposite spin near the crossing points in lifting the degeneracies, producing spin hybridized bands. This has the effect of creating a FS of mixed spin character. The

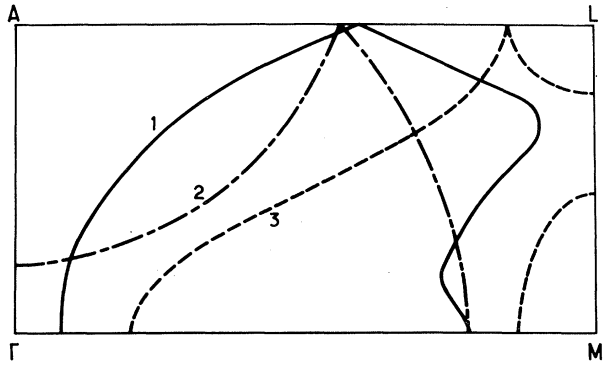

FIG. 8. Majority-electron Fermi surface cross sections in the ALM plane as found in different authors: ours (1), Wakoh and Yamashita (2) and Connolly (3).

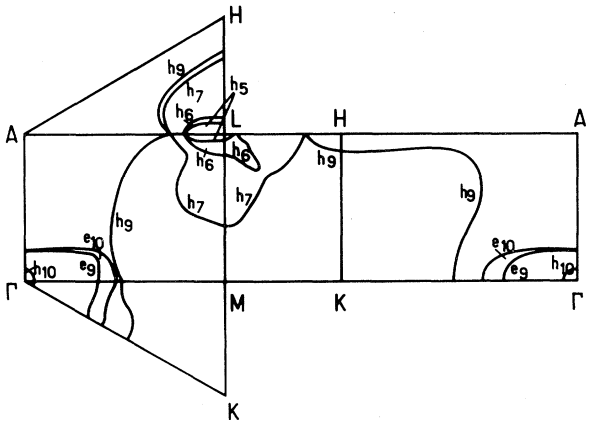

FIG. 9. Principal cross sections of the minority-electron Fermi surface when the spin-orbit interaction is qualitatively taken into account. The resulting splitting on the FS↓ in the ALH plane has also been represented.

resulting spin-hybridized FS is shown in Fig. 10.

In the presence of a weak magnetic induction $\vec{B}$, the electron will continue to turn in the hybridized portion, reversing regularly its spin orientation from ↑ to ↓ and vice versa. However, if $\vec{B}$ becomes sufficiently strong, the electron will have a finite probability to complete its primitive nonhybridized orbit by magnetic breakdown.

In an experiment, one would observe the hybridized FS of Fig. 10. With the presence of the magnetic induction suppressing some of the gaps, we return to the situation represented in Fig. 5. As we have introduced the s-o interaction only qualitatively, we do not know the actual width of the different gaps and thus do not know exactly the FS in a given experimental situation.

These gaps are very sensitive to the orientation of the magnetic induction and can possibly explain the anomalies observed in the amplitude of the dHvA effect in the ϵ frequency.[5] The same kind of anomalies have been observed in nickel[34] and iron.[35]

VI. MANY-BODY MASS ENHANCEMENT

In this section we attempt to analyze the various contributions to the many-body mass enhancement. An enchancement coefficient λ has been defined in Sec. V B from the specific-heat results. Here we define a λ such that for a given orbit

$$m^*/m_0 = 1 + \lambda , \tag{1}$$

where λ is the mass enhancement due to many-body effects. We consider the effects of three types of interactions: the electron-electron interaction, the electron-phonon interaction, and the electron-magnon interaction, which are characterized, respectively, by the coefficients λ_{e-e}, $\lambda_{e-\mathrm{ph}}$, and λ_{e-m}. λ_{e-e} is a Landau-type[36] coefficient, whereas $\lambda_{e-\mathrm{ph}}$ and λ_{e-m} can be considered generalized Landau-type[1,37] coefficients. As a first-order approximation the three effects can be considered as additive, so that the total mass enhancement can be written as

$$\lambda = \lambda_{e-e} + \lambda_{e-\mathrm{ph}} + \lambda_{e-m} . \tag{2}$$

A. The Γ neck

Let us now in particular look at the neck around Γ. In Sec. V C we have mentioned that the calculated transverse component of the band mass for this neck (defined by the FS↑) was

$$m_b/m_0 = 0.098 \pm 0.002 .$$

The measured cyclotron mass as given by the dHvA effect is

$$m^*/m_0 = 0.20 \pm 0.03 .$$

This gives a total enhancement of

$$\lambda = 1.04 \pm 0.35 .$$

In order to estimate the different contributions to λ, we have presented in Table V the various values of λ for the necks in the FS of cobalt, nickel, and copper. One notices first of all a large difference between the λ values for cobalt and nickel with those of copper. These differences arise from the fact that copper, unlike cobalt and nickel, is not a ferromagnet.

For the purpose of our analysis of cobalt we can safely neglect λ_{e-e}, in Eq. (2) as its value is much less than the uncertainty in our calculation.[36]

As we have seen in Sec. V C the Γ neck in the hcp cobalt FS↑ is topologically equivalent to the L neck in copper and nickel. Thus we use the copper value[38] of $\lambda_{e-\mathrm{ph}}$ for the Γ neck in cobalt, i.e.;

$$\lambda_{e-\mathrm{ph}}^{(\mathrm{neck})} = 0.23 \pm 0.05 .$$

This gives

$$\lambda_{e-m}^{(\mathrm{neck})} = 0.81 \pm 0.40 .$$

Now that we have an estimation of the λ components for a particular orbit, the Γ neck, the question is how to calculate the values of λ for the other parts of the cobalt FS. We cannot give a precise answer, but it is possible to make a realistic estimation in the following manner.

B. The λ values on the Fermi surface

1. *The electron-phonon mass enhancement*

For a given orbit, we can write for both Fermi surfaces the following relations[31,39]:

$$\lambda\uparrow_{e-\mathrm{ph},i} = N(E_F\uparrow)V_{e-\mathrm{ph},i} , \quad \text{for the FS}\uparrow \tag{3}$$

$$\lambda\downarrow_{e-\mathrm{ph},j} = N(E_F\downarrow)V_{e-\mathrm{ph},j} , \quad \text{for the FS}\downarrow , \tag{4}$$

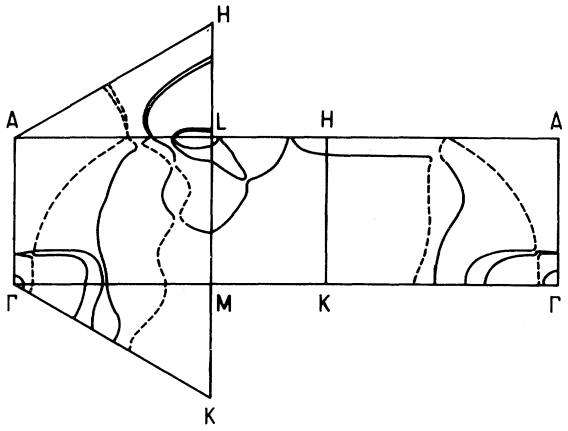

FIG. 10. Principal cross sections of the Fermi surface when spin hybridization is taken into account.

where i and j are orbit indexes.

The $V_{e-\mathrm{ph}}$ are matrix elements of the electron-electron interaction via the phonons, for a particular orbit. As a first estimation we consider $V_{e-\mathrm{ph}}$ as constant over the whole FS.[40]

As the FS↑ of cobalt corresponds to s-p type bands and has the same topological structure as that of copper (cf. Sec. V C) we take $\lambda\uparrow_{e-\mathrm{ph}}=0.12$ which is the value for the belly orbits in copper.[38]

The corresponding value $\lambda\downarrow_{e-\mathrm{ph}}$ for the FS↓ is then obtained from Eqs. (3) and (4):

$$\lambda\downarrow_{e-\mathrm{ph}}=0.34\,,$$

which is what one expects to get for a transition metal.[41]

2. The electron-magnon mass enhancement

To estimate the mass enhancement due to the electron-magnon interaction, we proceed in the same way as for the electron-phonon interaction. Although it is less clear due to the complexity of the electron-magnon interaction, it gives us a reasonable estimate.

Here too, we shall consider the matrix elements of the electron-electron interaction via the magnons[39] V_{e-m}, as a constant over the whole FS and then generalize the properties of a given orbit for both parts of the FS by writing

$$\lambda\uparrow_{e-m}=N(E_F\downarrow)V_{e-m}\,,\quad \text{for the FS}\uparrow \tag{5}$$

$$\lambda\downarrow_{e-m}=N(E_F\uparrow)V_{e-m}\,,\quad \text{for the FS}\downarrow\,. \tag{6}$$

It should be noticed that in these expressions the density of states corresponds to the direction of spin opposite to that for which λ_{e-m} is to be evaluated. This is due to the fact that V_{e-m} couples electrons with opposite spins.

As V_{e-m} is assumed to be constant we take

$$\lambda\uparrow_{e-m}=\lambda_{e-m}^{(\mathrm{neck})}=0.81\,.$$

$\lambda\downarrow_{e-m}$ is then obtained from expressions (5) and (6), and is found to be

$$\lambda\downarrow_{e-m}=0.31\,.$$

The resulting values for the total mass enhancement would then be for both parts of the FS:

$$\lambda\uparrow=0.93\,,$$

$$\lambda\downarrow=0.65\,.$$

On the other hand, we have seen in Sec. V B that the λ value obtained from specific-heat measurements was found to be

$$\lambda=0.74\,.$$

This value represents some kind of average on the whole FS, and we see that it falls in between $\lambda\uparrow$ and $\lambda\downarrow$, which is reasonable considering the approximations made.

VII. DISCUSSION

The physics of our particular one-electron formalism enters only through the effective potential $V(r)$, which is the potential of all the other electrons of the system (including exchange) as seen by a particular conduction electron. If the calculations were done self-consistently, the starting potential would be of little importance except to help reduce the number of iterations required to reach convergence. However, we were not programmed to do a self-consistent calculation and thus the particular choice of $V(r)$ plays an important role. Since we constructed our crystal potential from a superposition of atomic charge densities, it was necessary to choose an atomic configuration for Co which is appropriate for the atom when it sits in the crystal. We have chosen the atomic configuration $3d^74s^2$ as there is no experimental evidence as to the actual number of d electrons surrounding the nucleus in the crystal.

However, a more severe approximation which exists even in a self-consistent calculation is the choice of the exchange-correlation potential. We have used the local density approximation of the Kohn-Sham formalism.[20] This gave us an exchange-correlation potential proportional to $\alpha(\rho)^{1/3}$ where $\alpha=\frac{2}{3}$. As is well known, the coefficient α of this term has been used by some as a parameter to adjust the energy bands to obtain agreement with certain experiments (optical absorption spectra for example). A value of α greater than $\frac{2}{3}$ has the effect of narrowing and lowering the d bands with respect to the Fermi energy. The results of varying α are much greater on the energy bands than the particular choice of atomic configuration.

A more important problem which remains in ferromagnetic metals is the treatment of the ferromagnetic exchange. Several approaches have been

TABLE V. Many-body mass enhancement for the neck in the Fermi surface of cobalt, nickel, and copper.

	Orientation	Band mass m_b	m^*	λ
Co	⟨0001⟩	0.098 ± 0.002	0.20 ± 0.03 [a]	1.04 ± 0.35
Ni	⟨111⟩	0.13 ± 0.01 [b]	0.25 ± 0.02 [c]	0.92 ± 0.30
Cu	⟨111⟩	0.374 ± 0.01 [d]	0.46 ± 0.02 [e]	0.23 ± 0.05

[a] Reference 3.
[b] Reference 24.
[c] Reference 34.
[d] Reference 38.
[e] J. F. Koch, R. A. Stradling, and A. F. Kip, Phys. Rev. 133, A240 (1964).

made to include the exchange in the band calculations. One method using separate spin-dependent self-consistent potentials has been worked out for a first-principles calculation and was applied to iron[42] and nickel,[43] but with little success in explaining the experimental results. Another approach has been developed based on the Mueller-type interpolation scheme. It uses two additional parameters in order to characterize the ferromagnetic exchange splitting, and has succeeded in accurately describing the FS of nickel.[44] However, the two proceeding methods cannot give information about the origin of ferromagnetism. A particular method developed by Duff and Das,[45] who introduce an *ab initio* exchange correlation between spin-polarized bands, sheds some light on this problem. It was applied to iron but no clear conclusion could be drawn as to the validity of the results when comparison was made with experiment (essentially with the DOS).

We, on the other hand, have adopted the rigid-exchange-splitting approximation which is obtained by equating the number of spin-up and spin-down electrons to the experimental number of Bohr magnetons per atom. This is by far the simplest approximation possible and has been very successful in explaining the dHvA results especially for the large portions of the FS.[2]

Moreover, it can be shown quite easily that the Hamiltonian, including the rigid exchange splitting that we have used in this work, is nothing more than a simplified form of Hubbard's Hamiltonian.

The last point we wish to mention concerns the spin-orbit interaction. As we have seen it must be taken into account in order to explain the experimental results related to the FS$\downarrow$. Thus several of our results, in particular the orbits around L, are only qualitative. A quantitative treatment must necessarily take account of the noncommutative properties of the exchange and s-o operators and is beyond the scope of this work.

VIII. CONCLUSION

In this paper we have presented a band-structure calculation of ferromagnetic cobalt using a rigid exchange splitting.

Based on our results we have evaluated certain parameters used in the Stoner-Wohlfarth theory of ferromagnetism. An independent estimation of these values by Wohlfarth gave similar results showing that the essential features of our band structure agreed with the requirements of the itinerant-electron model.

The Fermi surface that we have calculated was in good agreement with the dHvA experiments, in particular for the neck at Γ (FS$\uparrow$) and for the interlaced pockets at L (FS$\downarrow$). For the latter, it was necessary to introduce spin-orbit coupling which was done, albeit in a qualitative way. This showed the necessity of including the s-o interaction for the full interpretation of the FS data.

Finally, a comparison with the existing experimental data had permitted us to estimate the mass enhancement due to many-body effects at the Γ neck. This included an estimate of the electron-magnon interaction. We have extended this result to the prediction of the mass enhancement on the whole FS.

ACKNOWLEDGMENT

The authors wish to thank Professor F. Mueller for his DOS computer program as well as for his helpful suggestions concerning the calculation.

---

*Laboratoire associé au Centre National de la Recherche Scientifique.

†Present address: Laboratoire de Physique des Solides, Bâtiment 510, Campus d'Orsay, 91401 Orsay, France.

[1]C. Herring, *Magnetism,* edited by G. T. Rado and H. Suhl (Academic, New York, 1966), Vol. IV.

[2]A. V. Gold, J. Low Temp. Phys. 16, 3 (1974).

[3]I. Rosenman and F. Batallan, Phys. Rev. B 5, 1340 (1972).

[4]J. R. Anderson, J. J. Hudak, and D. R. Stone, AIP Conf. Proc. 5, 477 (1972); 10, 46 (1973).

[5]F. Batallan and I. Rosenman, *Proceedings of the Thirteenth International Conference on Low Temperature Physics, Boulder, 1972,* edited by W. J. O'Sullivan, K. D. Timmerhaus, and E. F. Hammel (Plenum, New York, 1974).

[6]F. Batallan and I. Rosenman, Solid State. Commun. 12, 75 (1973).

[7]R. V. Coleman, R. C. Morris, and D. J. Sellmyer, Phys. Rev. A 8, 317 (1973).

[8]L. Hodges and H. Ehrenreich, J. Appl. Phys. 39, 1280 (1968).

[9]K. C. Wong, E. P. Wohlfarth, and D. M. Hum, Phys. Lett. A 29, 452 (1969).

[10]K. C. Wong, J. Phys. C 3, 378 (1970).

[11]S. Wakoh, Phys. Lett. A 31, 333 (1970).

[12]A. Y-C. Yu and W. E. Spicer, Phys. Rev. 167, 674 (1968).

[13]D. E. Eastman, J. Appl. Phys. 40, 1387 (1969).

[14]E. P. Wohlfarth, J. Appl. Phys. 41, 1205 (1970).

[15]J. D. Connolly, Intern. J. Quantum Chem. IIs, 257 (1968).

[16]S. Wakoh and J. Yamashita, J. Phys. Soc. Jpn. 28, 1151 (1970).

[17]S. Ishida, J. Phys. Soc. Jpn. 33, 369 (1972).

[18]C. Sommers and H. Amar, Phys. Rev. 188, 1117 (1969).

[19]C. Herring, J. Franklin Institute 233, 525 (1942).

[20]W. Kohn and L. J. Sham, Phys. Rev. A 137, 1697 (1965).
[21]J. P. Desclaux, CEA-CEN Limeil Report CEA-R-3929 (1970).
[22]The labeling of the sheets in the Fermi surfaces is the following: the symbols *e* and *h* are, respectively, for electrons and holes. The subscripts numbers are those of the corresponding Brillouin zone.
[23]R. J. Elliott, Phys. Rev. 96, 280 (1954).
[24]E. I. Zornberg, Phys. Rev. B 1, 244 (1970).
[25]R. Maglic and F. M. Mueller, Intern. J. Magnetism 1, 289 (1971).
[26]L. M. Falicov and M. H. Cohen, Phys. Rev. 130, 92 (1963).
[27]L. M. Falicov and J. Ruvalds, Phys. Rev. 172, 498 (1968).
[28]E. P. Wohlfarth, Rev. Mod. Phys. 25, 211 (1953).
[29]J. Kanamori, Prog. Theoret. Phys. 30, 275 (1963).
[30]C. H. Cheng, C. T. Wei, and P. A. Beck, Phys. Rev. 120, 426 (1960).
[31]G. Gladstone, M. A. Jensen, and J. R. Schrieffer *Superconductivity*, edited by R. D. Parks (Marcel Dekker, New York, 1969).
[32]L. F. Mattheiss, Phys. Rev. 151, 450 (1966).
[33]L. Hodges, D. R. Stone, and A. V. Gold, Phys. Rev. Lett. 19, 655 (1967).
[34]D. C. Tsui, Phys. Rev. 164, 669 (1967).
[35]D. R. Baraff, Phys. Rev. B 8, 3439 (1973).
[36]D. Pines and P. Nozières, *The Theory of Quantum Liquids* (Benjamin, New York, 1966).
[37]R. E. Prange and K. P. Kadanoff, Phys. Rev. 134, A566 (1964).
[38]M. J. G. Lee, Phys. Rev. B 2, 250 (1970).
[39]J. C. Phillips, *Proceedings of the International School of Physics "Enrico Fermi", Course XXXVII*, edited by W. Marshall (Academic, New York, 1967).
[40]A. J. Bennet, Phys. Rev. 140, 1902 (1965).
[41]W. L. MacMillan, Phys. Rev. 167, 331 (1968).
[42]S. Wakoh and J. Yamashita, J. Phys. Soc. Jpn. 21, 1712 (1966).
[43]J. W. D. Connolly, Phys. Rev. 159, 415 (1967).
[44]L. Hodges, H. Ehrenreich, and N. D. Lang, Phys. Rev. 152, 505 (1966).
[45]K. J. Duff and T. P. Das, Phys. Rev. B 3, 192 (1971).